

## Electronic Supplementary Information (ESI)

### High-sensitive friction-imaging devices based on cascading stimuli responsiveness

Nano Shioda,<sup>a</sup> Ryotaro Kobayashi,<sup>b</sup> Seiichiro Katsura,<sup>b</sup> Hiroaki Imai,<sup>a</sup> Syuji Fujii,<sup>\*,c</sup> Yuya Oaki<sup>\*,a</sup>

<sup>a</sup> Department of Applied Chemistry, Faculty of Science and Technology, Keio University, 3-14-1 Hiyoshi, Kohoku-ku, Yokohama 223-8522, Japan.

<sup>b</sup> Department of System Design Engineering, Faculty of Science and Technology, Keio University, 3-14-1 Hiyoshi, Kohoku-ku, Yokohama 223-8522, Japan.

<sup>c</sup> Department of Applied Chemistry, Faculty of Engineering, Osaka Institute of Technology, 5-16-1 Omiya, Asahi-ku, Osaka 535-8585, Japan

\*E-mail: syuji.fujii@oit.ac.jp, oakiyuya@applc.keio.ac.jp

### Contents

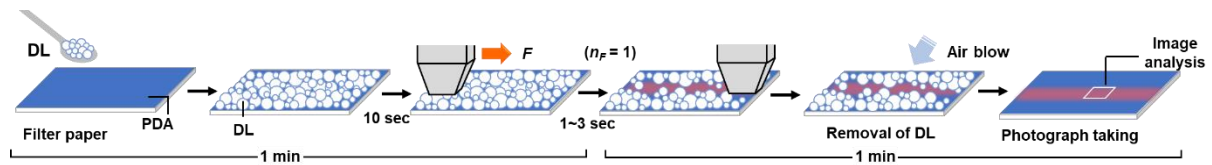
|   |        |
|---|--------|
| Experimental methods (Scheme S1)  | P. S3  |
| Previous works about quantitative detection of friction forces (Fig. S1)  | P. S5  |
| SEM image and Raman spectra of the PDA-coated paper (Fig. S2)             | P. S6  |
| Particle-size distribution, composition, and morphology of DL (Fig. S3)   | P. S7  |
| Enhanced sensitivity of PDA/DL (Fig. S4)                                  | P. S9  |
| Experimental setup for the application of friction forces (Fig. S5)       | P. S10 |
| Estimation method of the applied $F$ (Fig. S6)                            | P. S11 |
| Photographs with the application of friction force (Fig. S7 and Table S1) | P. S13 |
| Changes in friction coefficient (Fig. S8)                                 | P. S15 |
| Sensitivity tuning (Figs. S9, S10 and Tables S3–S5)                       | P. S16 |
| Reference devices using the different substrates (Fig. S11)               | P. S18 |
| Application of simulated unknown friction force (Fig. S12 and Table S6)   | P. S19 |

|  |        |
|--|--------|
| Reference experiments using c-DL (Fig. S13 and Table S7)           | P. S20 |
| Weight of the collapsed DLs (Table S8)                             | P. S21 |
| Reference devices using the different substrates (Fig. S14)        | P. S22 |
| Color-changing behavior of PDA and PDA/DL (Fig. S15)               | P. S23 |
| Application of unknown friction force (Fig. S16 and Table S9)      | P. S24 |
| Application of unknown friction force in calligraphy (Fig. S17)    | P. S25 |
| Force-distribution mapping using a rigid undeformed pen (Fig. S18) | P. S26 |

## Experimental methods

**Preparation of the PDA/DL device.** A piece of commercial filter paper 25 mm × 25 mm in size (Advantec, quantitative grade, No. 5C) was dipped in the precursor chloroform solution containing 10 mg cm<sup>-3</sup> 10,12-pentacosadiynoic acid (PCDA, TCI, 97.0%) for 5 sec. The PCDA-coated paper was dried at room temperature and polymerized with irradiation of UV light (6 W, UV lamp, 254 nm). DL was produced by the method according to our previous reports.<sup>54–56</sup> An aqueous solution containing 20 wt% polyethylenimine (PEI, Nippon Shokubai, branched chain with  $\bar{M}_n = 300$ ) (25 cm<sup>3</sup>) and hydrophobic surface-modified silica particles with polydimethylsiloxane (PDMS-SiO<sub>2</sub>, Aerosil RY-300, 21–27 nm in diameter) (2.78 g) were mixed at 20000 rpm for 5 sec using a mixer. The resultant DL was selected using stainless sieves with the pore sizes of 105 and 250 μm and stored in a sealed polypropylene bottle until the use. DL with two cups of spatula, average 7.58 mg, were homogeneously dispersed on the rectangular area (2.5 mm × 20 mm) of the cut PDA-coated paper device (5 mm × 25 mm in size).

**Imaging and measuring the applied friction force.** The application of friction forces was performed within 10 s at a constant speed after the preparation of the device (Scheme S1). The remaining DLs were immediately removed by air blow. The photographs of the PDA/DL device were taken using a smartphone (iPhone 13) to estimate the red-color intensity  $x$ .



**Scheme S1.** Schematic illustrations of the processes from the device setting to photograph taking.

The initial  $x$  ( $x_0$ ) of each device measured before loading DL. The  $x$  value was calculated by an international standard (Eqs. S1 and S2) using RGB values of the photographs.<sup>57</sup>

$$\begin{bmatrix} X \\ Y \\ Z \end{bmatrix} = \begin{bmatrix} 0.4124 & 0.3576 & 0.1805 \\ 0.2126 & 0.7152 & 0.0722 \\ 0.0193 & 0.1192 & 0.9505 \end{bmatrix} \begin{bmatrix} R \\ G \\ B \end{bmatrix} \quad \dots \text{(Eq. S1)}$$

$$(x, y) = \left( \frac{X}{X+Y+Z}, \frac{Y}{X+Y+Z} \right) \quad \dots \text{(Eq. S2)}$$

Friction force was applied to the PDA/DL device using a handmade mount with four legs (18 g) and weights (0, 20, 50, 100, 150, 200, 300 g) (see Fig. S5 in the ESI). The applied normal force ( $N$ ) was measured using a platform scale set under the device. The applied friction force ( $F$ ) was measured using a spring scale. The friction coefficient was calculated by  $N$  and  $F$ . Friction force was applied to the device once with drawing the mount and weight one way. The remaining DL on the device was removed using a handy blower. The red-color intensity ( $x$ ) was measured at 1 min after the application of friction force to estimate an increment of  $x$ ,  $\Delta x (= x - x_0)$ . The image analysis was carried out on the area  $0.5 \text{ mm} \times 1.5 \text{ mm}$  of the device. The relationship between  $F$  and  $\Delta x$  was measured on four samples to ensure the reproducibility of the standard curve (Fig. S7 in the ESI).

Unknown friction force was applied using an ornament of giant panda. The ornament with four feet in the different contact states on the table was drawn on the device using a spring scale. Handwriting in calligraphy was performed three times on the PDA/DL device using the same brush without ink by expert (R. K., second author), experienced (N. S., first author), and inexperienced (Y. H., a student in the authors' group). The  $\Delta x$  values in each stroke were analyzed by the photographs of the original and color-changed devices dividing into 62 domains ( $0.5 \text{ mm} \times 0.5 \text{ mm}$ ).

Force sensor (Tec Gihan, USL06-H5) was used to analyze the applied forces by hand to brush in the lateral and vertical directions.<sup>58</sup> The sensor was embedded in the brush for calligraphy. The expert wrote the same character with gripping the sensor as shown in Fig. S16a.

**Structural characterization.** The PDA/DL devices were observed using a field-emission scanning electron microscopy (SEM, Carl-Zeiss MERLIN VP compact) with energy-dispersive X-ray analysis (EDX, Bruker XFlash), optical microscopy (Keyence, VHX-1000), and X-ray computer tomography (XCT, Shimadzu XDimensus 300). The intercalation behavior of PEI in the layered PDA was analyzed by X-ray diffraction (XRD, Bruker D8-Advance) and Fourier transform infrared (FT-IR, JASCO FT/IR-4200) spectroscopy using the KBr method. Raman (Renishaw InVia Raman, excitation light: 785 nm) and UV-Vis (Jasco V-670) were used to analyze the torsional behavior of the PDA main chain.

## Previous works about quantitative detection of friction forces

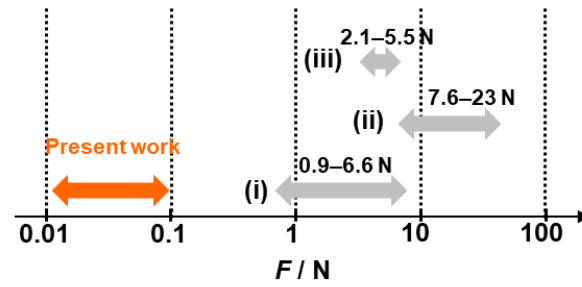


**Fig. S1.** Quantitation range of friction forces in the previous works.<sup>48–50</sup>

Although the qualitative visualization of friction force was achieved in previous works,<sup>7–16</sup> the quantitative measurement was not fully studied except a couple of the previous works.<sup>48–50</sup> Friction forces stronger than 1 N were quantified in previous works (i), (ii), and (iii) corresponding to the references 48, 49, and 50, respectively. However, the friction force weaker than 1 N was not detected.

## SEM image and Raman spectra of the PDA-coated paper

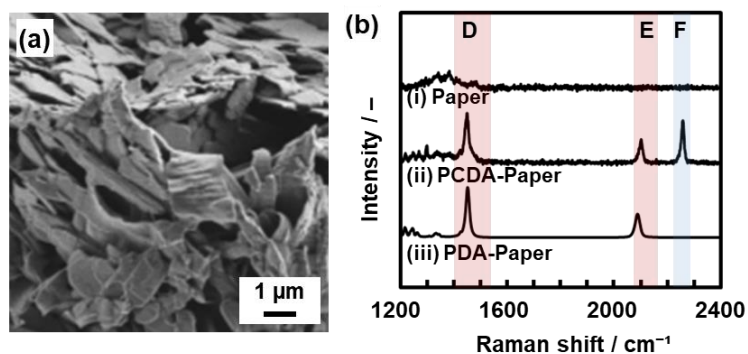


**Fig. S2.** PDA-coated filter paper. (a) SEM image of the PDA sheets coated on a filter paper. (b) Raman spectra of a pristine filter paper (i), monomer PCDA-coated paper (ii), and PDA-coated paper (iii).

The lateral size and thickness of the PDA sheets was around 1 μm and 150 nm, respectively (Fig. S2a). The peak corresponding C≡C bond of the monomeric DA moiety was observed around 2250 cm<sup>-1</sup> (band F in Fig. S2b). The peaks characteristic to ene-yne structure of PDA main chain were only observed around 1450 and 2100 cm<sup>-1</sup> after the polymerization (bands D and E in Fig. S2b, respectively). The Raman spectra supported the polymerization of PCDA.

## Particle-size distribution, composition, and morphology of DL

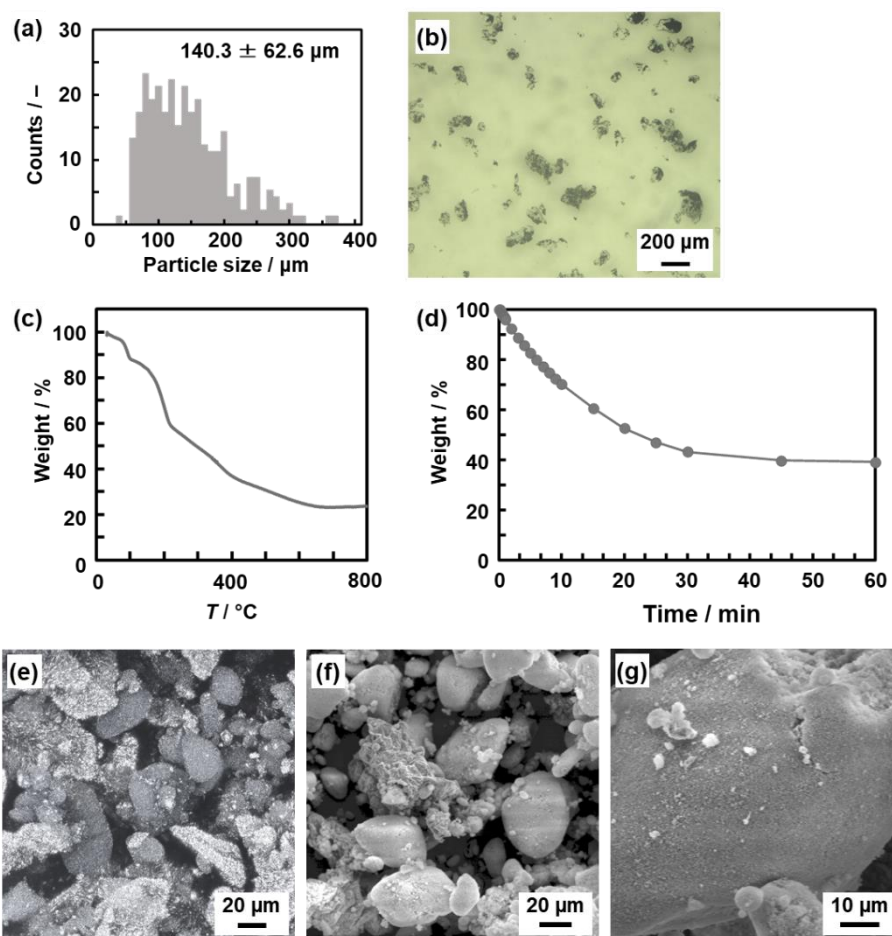


**Fig. S3.** Structural characterization of DLs after sieving. (a) Particle size distribution (the number of samples:  $n = 300$ ). (b) Representative optical microscopy image to measure the particle size. (c) Thermogravimetry (TG) curve of DL under air atmosphere. (d) Time-dependent weight decrease of DLs at room temperature under ambient pressure. (e) Laser microscopy (LM) image with the focus stacking. (f,g) SEM images of DLs.

Although the particle size was selected using a stainless sieve with the pore sizes of 105 and 250  $\mu\text{m}$ , the smaller and larger particles were included. The size was measured by Image J software. The average size  $140.3 \pm 62.6 \mu\text{m}$  was measured based on the longitudinal size. The TG curve indicates that DLs contain 76.2 wt% of PEI aqueous solution as the interior liquid (Fig. S3c). When the DLs were maintained at room temperature under ambient pressure, 60.9 % of PEI and  $\text{SiO}_2$  remained after the evaporation of water (Fig. S3d). These results indicate that the composition of DL was 23.8 wt% for  $\text{SiO}_2$ , 15.4 wt% for PEI, and 60.9 wt% for water. LM image showed the irregular shape of the DLs containing the interior liquid (Fig. S3e). The

similar irregular non-spherical particle morphology was observed by SEM even though the interior water was evaporated under the vacuum condition. These non-spherical droplets are formed to stabilize the interface by fusion of two or more droplets with the partial coating of SiO<sub>2</sub>. As the SiO<sub>2</sub> particles adsorb on the air-liquid interface in the crowded state, the further coalescence with the rearrangement of the SiO<sub>2</sub> particles is not easily achieved. The non-spherical droplets were observed in the particle-stabilized emulsion,<sup>S1,S2</sup> bubble,<sup>S3</sup> and liquid marble systems.<sup>S4</sup>

#### **Additional references**

- S1. J.-W. Kim, D. Lee, H. C. Shum and D. A. Weitz, *Adv. Mater.*, 2008, **20**, 3239.
- S2. S. Fujii, Y. Yokoyama, Y. Miyanari, T. Shiono, M. Ito, S. Yusa and Y. Nakamura, *Langmuir*, 2013, **29**, 5457.
- S3. A. B. Subramaniam, M. Abkarian, L. Mahadevan and H. A. Stone, *Nature*, 2005, **438**, 930.
- S4. X. Li, Y. Xue, P. Lv, H. Lin, F. Du, Y. Hu, J. Shen and H. Duan. *Soft Matter*, 2016, **12**, 1655.



**Enhanced sensitivity of PDA/DL**

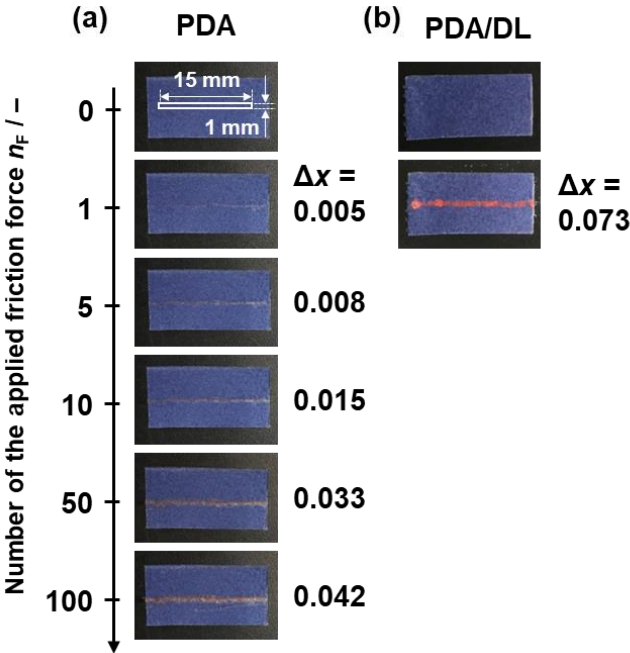


**Fig. S4.** Photographs of PDA (a) and PDA/DL (b) with the application of the same friction force.

The applied normal force was measured to be 4.9 N using a balance set under the PDA-coated device. At  $n_F = 1$ ,  $\Delta x$  of PDA/DL was larger than that of PDA. Although  $\Delta x$  of PDA increased up to 0.042 at  $n_F = 100$ , the  $\Delta x$  value was smaller than that of PDA/DL at  $n_F = 1$ .

## Experimental setup for the application of friction forces

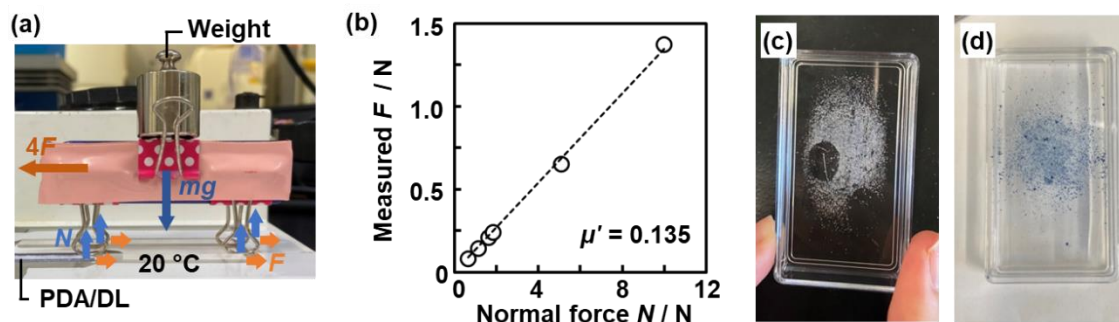


**Fig. S5.** Experimental setup for the application of friction force and its reference experiment. (a) Photograph of a weight and handmade mount to apply friction force to the device. (b) Relationship between  $N$  and  $F$  measured using a platform scale and spring scale, respectively. (c,d) Photographs of DL (c) and PDA (d) powders adsorbed on the electrified surface of a polystyrene substrate.

The different  $F$  was achieved by changes in the weights (0, 20, 50, 100, 150, 200, and 300 g) on the base with four legs (18 g) (Fig. S5a). The actual  $F$  was measured using a spring scale attached on the base (Fig. S5b). The friction coefficient was estimated to  $\mu' = 0.135$  from the relationship between  $N$  and  $F$  (Fig. S5b). Although the powders of DL and PDA were adsorbed on the electrified surface, the disruption of DL and color change of PDA were not observed (Fig. S5c,d).

## Estimation method of the applied $F$

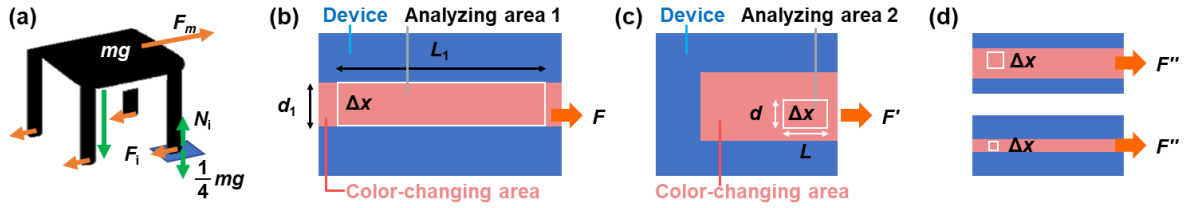


**Fig. S6.** Protocol for colorimetric estimation of the applied friction forces. (a) An object with four legs applying friction force. (b–d) Schematic illustrations of the device size (blue), color-changing area (red), and analyzing areas 1 and 2 (white).

The relationship between  $F$  and  $\Delta x$  was prepared as the calibration curve (Fig. 2k). Friction force was applied to the PDA/DL devices by the four equivalent legs (Figs. S5a and S6a), where  $m$  is weight and  $g$  is gravity acceleration. The overall friction force ( $F_m$ ) was measured by a spring scale (Fig. S5b). The measured  $F_m$  and individual friction force ( $F_i = F$ ) have the following relationship (Eq. S3) (Fig. S6a).

$$F_m = 4 F_i \quad \dots \text{(Eq. S3)}$$

After  $F$  in the range of 0.006–0.105 N was applied, the image analysis was carried out in the analyzing area 1 ( $d_1 \times L_1$ ,  $d_1 = 0.5$  mm,  $L_1 = 15$  mm) to estimate  $\Delta x$  (Fig. S6b). As the  $\Delta x$  value means the ratio of the color-changed pixels without the blue blank space in the image regardless of the area, the relationship between  $F$  and  $\Delta x$  can be applied to estimate unknown friction forces ( $F'$ ) in the different analyzing area 2 ( $d \times L$ ) because of the following reasons (Fig. S6c).

Friction forces provide accumulation of the work to the molecules, such as torsion of the conjugated main chain and disruption of the layered structure, in the analyzing area 1. As the amount of the loaded molecules depends on the area ( $d_1 \times L_1$ ), the work applied with  $F$  is described by the left-hand side of (Eq. S4). On the other hand, the overall chromaticity changes in the area 1 is described by the right-hand side of (Eq. S4). The accumulated work has a proportional relationship with the chromaticity change.

$$F \times d_1 \times L_1 \propto \Delta x \times d_1 \times L_1 \quad \dots \text{(Eq. S4)}$$

Therefore, the linear relationship between  $F$  and  $\Delta x$  is described by (Eq. S5) using constants  $a$  and  $b$  specific to the device.

$$F = a\Delta x + b \dots \text{(Eq. S5)}$$

The  $\Delta x$  values mean the ratio of the color-changed pixels in the color-changed area applied by friction force without the blue blank space around the stressed part (Fig. S6c). The relationship between  $F$  and  $\Delta x$  (Eq. S5), *i.e.* the standard curve in Fig. 2k, can be applied to estimate unknown  $F'$  applied in the different area.

When the friction force  $F''$  is applied to the device using the different objects with the different contact areas (Fig. S6d),  $F''$  can be estimated from the  $\Delta x$  values in any analyzing area (white squares) without including the blue blank space. The  $\Delta x$  values represent the ratio of the color-changed pixels originating from the applied friction force. The  $\Delta x$  value is ideally the same in any red-colored area.

## Photographs with the application of friction force

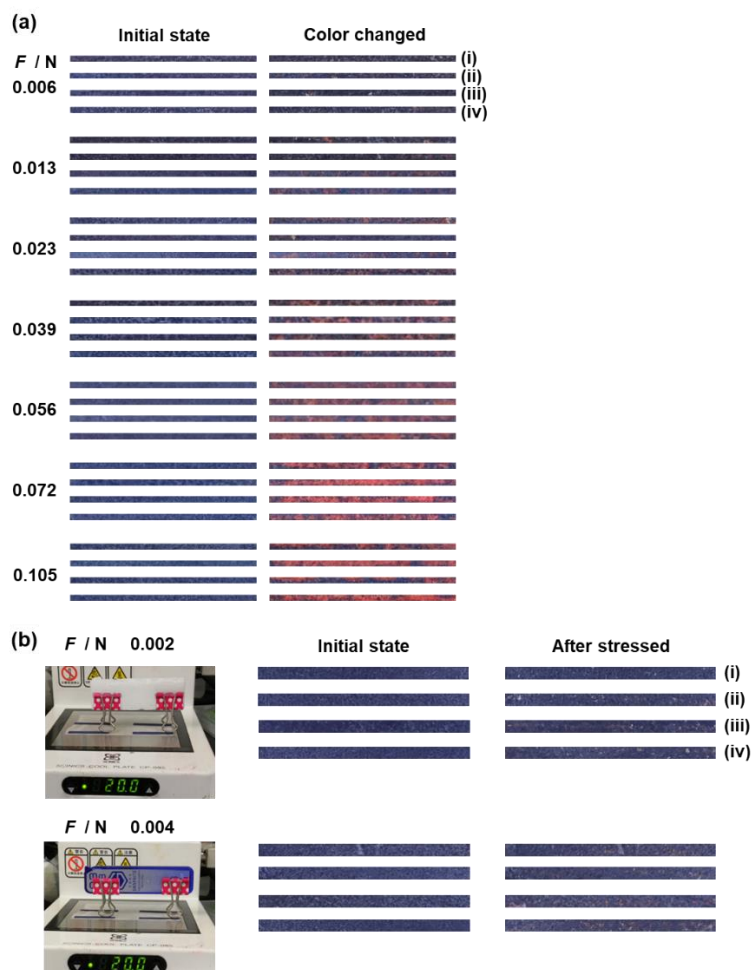


**Fig. S7.** Photographs of the initial state (left) and stressed state with the application of friction force  $F = 0.006\text{--}0.105$  N (a) and 0.002 and 0.004 N (b) on PDA/DL in the range of 105–250  $\mu\text{m}$  (right) for the trials (i)–(iv).

**Table S1.** Summary of  $F$  and  $\Delta x$  for PDA/DL in the range of 105–250  $\mu\text{m}$ .

| $F / \text{N}$            | 0.0059 | 0.0125 | 0.0225 | 0.0390 | 0.0556 | 0.0721 | 0.1052 |
|---------------------------|--------|--------|--------|--------|--------|--------|--------|
| (i) $\Delta x / -$        | 0.0054 | 0.0081 | 0.0241 | 0.0287 | 0.0406 | 0.0757 | 0.0583 |
| (ii) $\Delta x / -$       | 0.0093 | 0.0093 | 0.0037 | 0.0389 | 0.0423 | 0.0597 | 0.0790 |
| (iii) $\Delta x / -$      | 0.0072 | 0.0138 | 0.0142 | 0.0372 | 0.0362 | 0.0756 | 0.0861 |
| (iv) $\Delta x / -$       | 0.0075 | 0.0174 | 0.0256 | 0.0354 | 0.0503 | 0.0540 | 0.0507 |
| $\overline{\Delta x} / -$ | 0.0073 | 0.0121 | 0.0169 | 0.0350 | 0.0424 | 0.0663 | 0.0685 |
| S. D. / -                 | 0.0014 | 0.0037 | 0.0088 | 0.0039 | 0.0051 | 0.0096 | 0.0145 |

The experiment was carried out four times (i)–(iv). The standard curve in Fig. 2k was prepared based on these data. The different setup was prepared to apply  $F$  lower than 0.006 N (photographs in Fig. S7b). The color change was not observed for the naked eye at  $F = 0.004$  and 0.002 N.

## Changes in friction coefficient

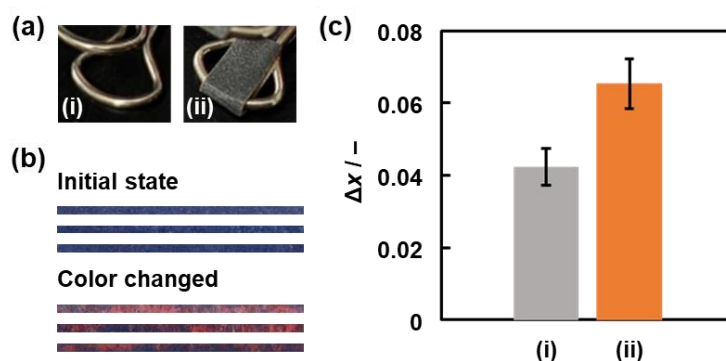


**Fig. S8.** Application of friction forces with changes in the friction coefficient. (a) Photographs of the standard contact state (i, left) and its reference with attaching a sandpaper on the bottom of the leg (ii, right). (b) Photographs of the initial state (upper) and color-changed state with the application of friction force by the setup (ii) (lower). (c) Differences in the  $\Delta x$  values of the setups (i) and (ii).

The same weight (150 g) was used for the setups (i) and (ii). The friction coefficient of the setups (i) and (ii) was 0.135 and 0.190, respectively. The average  $\Delta x$  values of the setups (i) and (ii) were  $0.042 \pm 0.0044$  and  $0.065 \pm 0.069$ , respectively (Fig. S8c).

## Sensitivity tuning

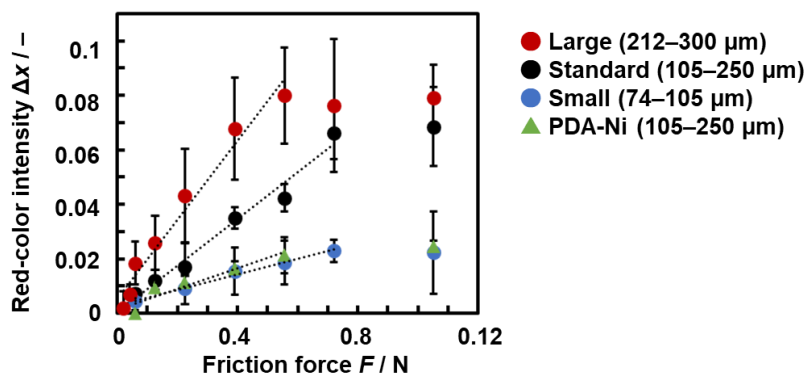


**Fig. S9.** Relationship between  $F$  and  $\Delta x$  of PDA/DL using the different particle-size distribution of DLs and  $Ni^{2+}$ -intercalated PDA (PDA- $Ni^{2+}$ )/DLs with the standard particle-size distribution.

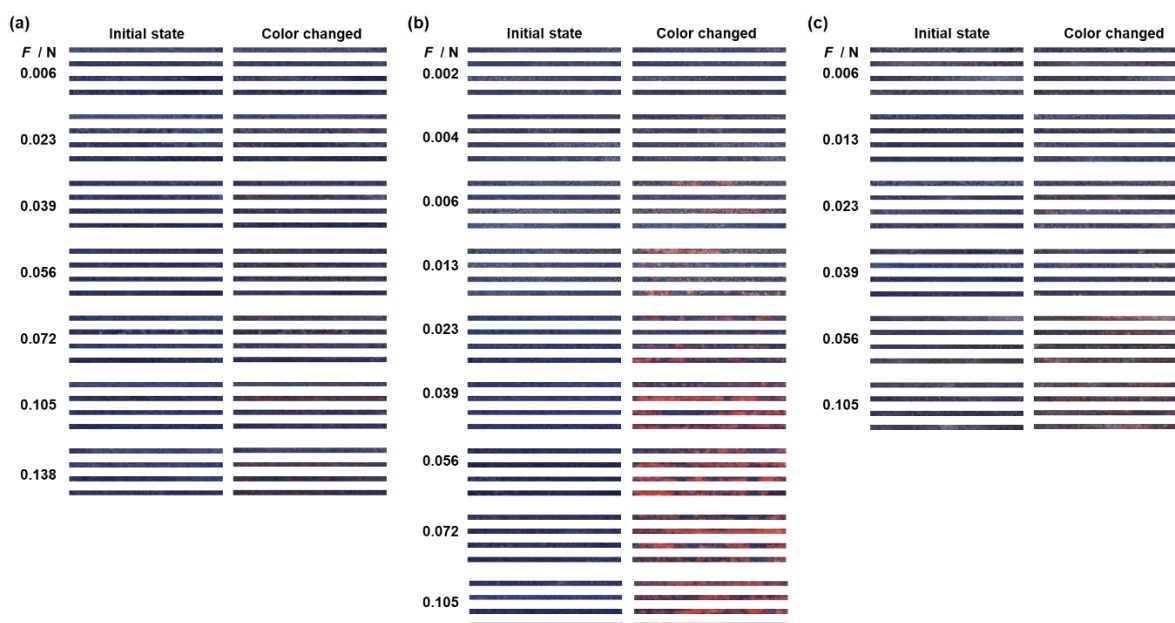


**Fig. S10.** Photographs of the initial state (left) and color-changed state with the application of friction forces by changing the particle-size distribution in the range of 74–105  $\mu m$  (a), and 212–300  $\mu m$  (b) and PDA- $Ni^{2+}$  with DLs in the range of 105–250  $\mu m$  (c).



**Table S3.** Summary of  $F$  and  $\Delta x$  for PDA/DL with DLs in the range of 74–105  $\mu\text{m}$ .

| $F/N$                     | 0.0059 | 0.0225 | 0.0390 | 0.0556 | 0.0721 | 0.1052 | 0.1383 |
|---------------------------|--------|--------|--------|--------|--------|--------|--------|
| (i) $\Delta x / -$        | 0.0027 | 0.0047 | 0.0125 | 0.0278 | 0.0147 | 0.0084 | 0.0054 |
| (ii) $\Delta x / -$       | 0.0040 | 0.0181 | 0.0292 | 0.0215 | 0.0215 | 0.0475 | 0.0423 |
| (iii) $\Delta x / -$      | 0.0069 | 0.0096 | 0.0145 | 0.0255 | 0.0223 | 0.0192 | 0.0350 |
| (iv) $\Delta x / -$       | 0.0040 | 0.0038 | 0.0053 | 0.0170 | 0.0128 | 0.0141 | 0.0287 |
| $\overline{\Delta x} / -$ | 0.0044 | 0.0090 | 0.0154 | 0.0187 | 0.0230 | 0.0223 | 0.0279 |
| S. D.                     | 0.0015 | 0.0057 | 0.0087 | 0.0079 | 0.0041 | 0.0151 | 0.0138 |

**Table S4.** Summary of  $F$  and  $\Delta x$  for PDA/DL with DLs in the range of 212–300  $\mu\text{m}$ .

| $F/N$                     | 0.0020  | 0.0042 | 0.0059 | 0.0125 | 0.0225 | 0.0390 | 0.0556 | 0.0721 | 0.1052 |
|---------------------------|---------|--------|--------|--------|--------|--------|--------|--------|--------|
| (i) $\Delta x / -$        | 0.0092  | 0.0125 | 0.0250 | 0.0362 | 0.0514 | 0.0376 | 0.0496 | 0.0478 | 0.0795 |
| (ii) $\Delta x / -$       | 0.0014  | 0.0057 | 0.0131 | 0.0141 | 0.0163 | 0.0872 | 0.0934 | 0.1126 | 0.0722 |
| (iii) $\Delta x / -$      | -0.0077 | 0.0026 | 0.0272 | 0.0179 | 0.0426 | 0.0677 | 0.0865 | 0.0834 | 0.0984 |
| (iv) $\Delta x / -$       | 0.0044  | 0.0077 | 0.0083 | 0.0352 | 0.0628 | 0.0789 | 0.0901 | 0.0616 | 0.0662 |
| $\overline{\Delta x} / -$ | 0.0018  | 0.0071 | 0.0184 | 0.0258 | 0.0433 | 0.0678 | 0.0799 | 0.0763 | 0.0791 |
| S. D.                     | 0.0062  | 0.0036 | 0.0079 | 0.0099 | 0.0171 | 0.0188 | 0.0177 | 0.0245 | 0.0121 |

**Table S5.** Summary of  $F$  and  $\Delta x$  for PDA-Ni<sup>2+</sup> with DLs in the range of 105–250  $\mu\text{m}$ .

| $F/N$                     | 0.0059  | 0.0125 | 0.0225 | 0.0390 | 0.0556 | 0.1052 |
|---------------------------|---------|--------|--------|--------|--------|--------|
| (i) $\Delta x / -$        | -0.0019 | 0.0094 | 0.0089 | 0.0131 | 0.0211 | 0.0226 |
| (ii) $\Delta x / -$       | 0.0000  | 0.0104 | 0.0147 | 0.0183 | 0.0314 | 0.0264 |
| (iii) $\Delta x / -$      | 0.0013  | 0.0095 | 0.0124 | 0.0145 | 0.0128 | 0.0269 |
| (iv) $\Delta x / -$       | 0.0008  | 0.0081 | 0.0090 | 0.0199 | 0.0204 | 0.0219 |
| $\overline{\Delta x} / -$ | 0.0001  | 0.0094 | 0.0112 | 0.0165 | 0.0214 | 0.0245 |
| S. D.                     | 0.0012  | 0.0008 | 0.0025 | 0.0027 | 0.0066 | 0.0022 |

A paper substrate with coating PDA-Ni<sup>2+</sup> was prepared by the procedure in our previous report.<sup>56</sup> The sensitivity is changed to 0.33 times for the small DL, 1.70 times for the larger DL, and 0.44 times for PDA-Ni<sup>2+</sup> based on the slope on the assumption that the slope of PDA/DL (standard) is 1.00 in the range of  $0 < F < 0.56$  (Fig. S9).

## Spatial resolution of the PDA/DL device

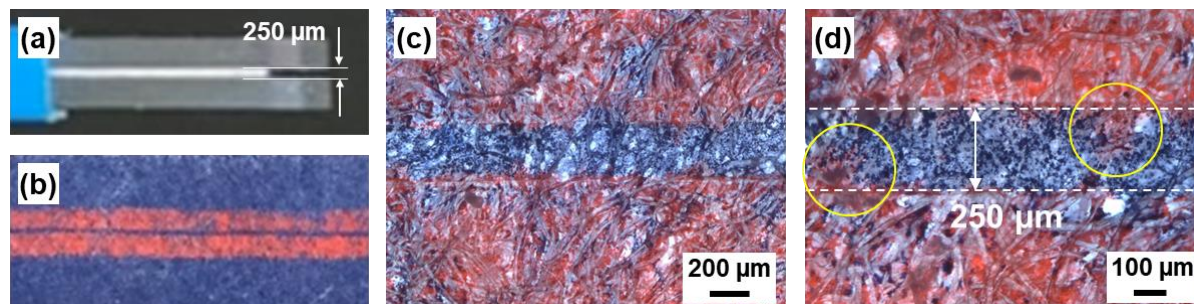


**Fig. S11.** Application of the friction force using the two metal objects with the distance between 250 μm. (a) A paper holding with two metal blocks to ensure the distance 250 μm. (b) A photograph with the application of the friction force using the object as shown in Fig. S11a. (c,d) Magnified optical microscopy images of the device.

The photographs show that the device ensured the spatial resolution around 250 μm (Fig. S11b,c). However, the red-color domain slightly exuded the unstressed area (the yellow circles in Fig. S11d).

## Application of simulated unknown friction force

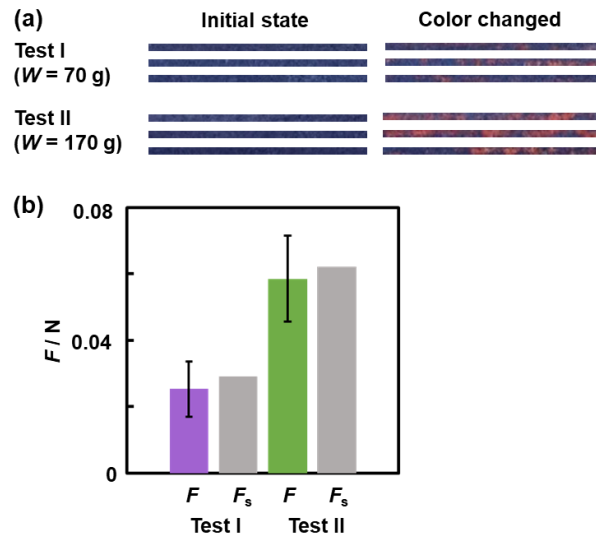


**Fig. S12.** Application of simulated unknown friction forces using weight 70 g for Test I and 170 g for Test II. (a) Photographs of the initial state (left) and color-changed states with the application of simulated unknown friction forces (right). (b) Estimated  $F$  from  $\Delta x$  for Tests I (purple) and II (green) and  $F_s$  measured using a spring scale for Tests I and II (gray).

**Table S6.** Summary of  $F$  and  $\Delta x$  for Tests I and II.

|                           | Test I<br>( $W = 70$ g) | Test II<br>( $W = 170$ g) |
|---------------------------|-------------------------|---------------------------|
| (i) $\Delta x / -$        | 0.01741                 | 0.04199                   |
| (ii) $\Delta x / -$       | 0.03087                 | 0.06419                   |
| (iii) $\Delta x / -$      | 0.01782                 | 0.04525                   |
| $\overline{\Delta x} / -$ | 0.02203                 | 0.05048                   |
| S. D. / -                 | 0.00625                 | 0.00979                   |
| Estimated $F / \text{N}$  | 0.02528                 | 0.05851                   |
| $F_s / \text{N}$          | 0.02908                 | 0.06218                   |

## Reference experiments using c-DL

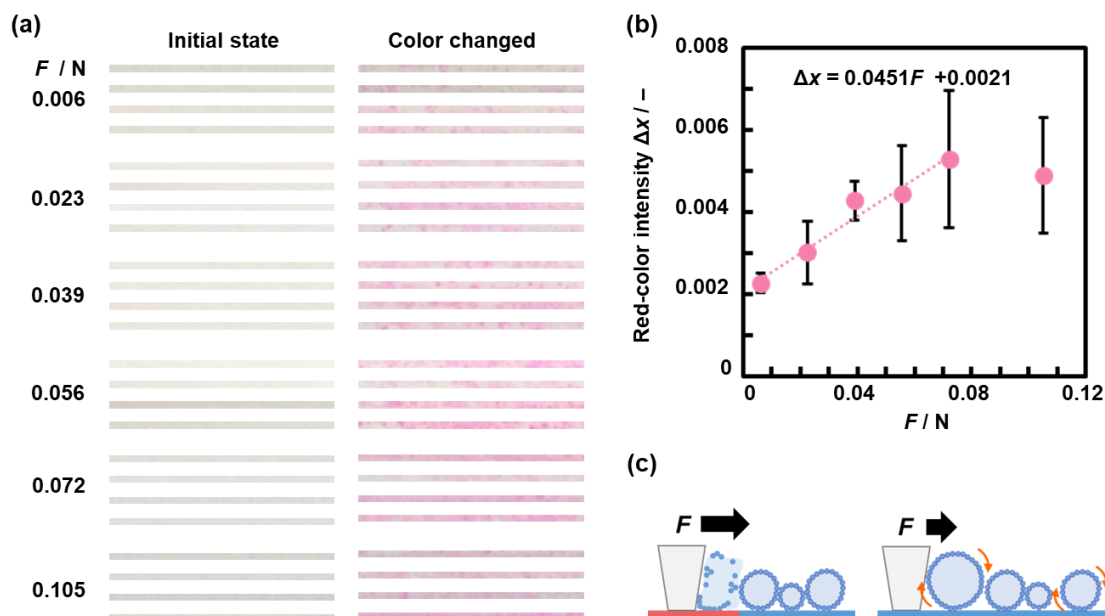


**Fig. S13.** Response of the reference device with dispersion of the c-DL on a paper substrate without coating PDA. (a) Photographs of the initial state (left) and color-changed states with the application of friction forces on the reference device (right). (b) Relationship between  $F$  and  $\Delta x$  for the reference device. (c) Schematic illustration of the disruption behavior of DLs under the larger (left) and smaller (right)  $F$ .

**Table S7.** Summary of  $F$  and  $\Delta x$  for the reference device.

| Ideal $F/N$               | 0.0059 | 0.0225 | 0.0390 | 0.0556 | 0.1052 |
|---------------------------|--------|--------|--------|--------|--------|
| (i) $\Delta x / -$        | 0.0019 | 0.0024 | 0.0040 | 0.0046 | 0.0061 |
| (ii) $\Delta x / -$       | 0.0023 | 0.0034 | 0.0044 | 0.0029 | 0.0024 |
| (iii) $\Delta x / -$      | 0.0024 | 0.0041 | 0.0050 | 0.0043 | 0.0063 |
| (iv) $\Delta x / -$       | 0.0025 | 0.0023 | 0.0037 | 0.0061 | 0.0063 |
| $\overline{\Delta x} / -$ | 0.0023 | 0.0030 | 0.0043 | 0.0045 | 0.0053 |
| S. D. / -                 | 0.0002 | 0.0008 | 0.0005 | 0.0012 | 0.0017 |

Whereas the larger  $F$  induces the disruption DLs, the rolled DLs under the smaller  $F$  remains without the disruption (Fig. S13c).

## Weight of the collapsed DLs

**Table S8.** Weight of the collapsed DLs ( $W_{\text{col-DL}}$ ) depending on  $F$ .

| $F / \text{N}$                        | 0.006 | 0.039 | 0.072 |
|---------------------------------------|-------|-------|-------|
| $W_{\text{col-DL (i)}} / \text{mg}$   | 1.0   | 1.4   | 2.3   |
| $W_{\text{col-DL (ii)}} / \text{mg}$  | 1.1   | 1.5   | 2.1   |
| $W_{\text{col-DL (iii)}} / \text{mg}$ | 1.3   | 1.8   | 2.2   |
| Average / mg                          | 1.1   | 1.6   | 2.2   |
| S. D. / mg                            | 0.12  | 0.17  | 0.08  |

The initial PDA/DL device loaded ( $W_{\text{DL}} =$ ) 7.6 mg of DL. After the friction force applied, the remaining DL on the device was collected to measure the weight ( $W_{\text{DL}'}$ ). The differences between  $W_{\text{DL}}$  and  $W_{\text{DL}'}$  correspond to  $W_{\text{col-DL}}$  in Table S8.  $W_{\text{col-DL}}$  increased with increasing  $F$ .

## Reference devices using the different substrates

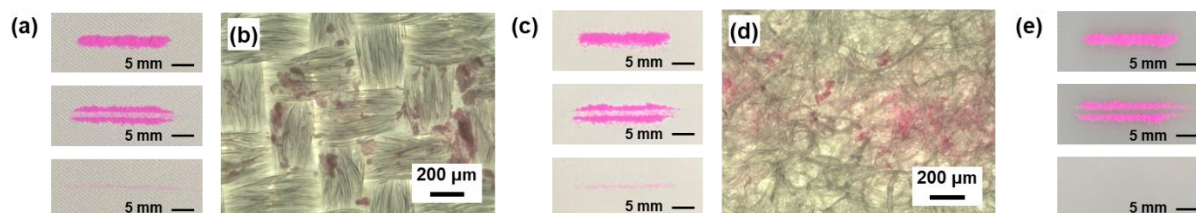


**Fig. S14.** Color-change behavior of the reference devices prepared using c-DLs and different substrates. (a) Silk cloth with the rough surface. (b) Filter paper used in the present work. (c) Polycarbonate with the smooth surface. (a,c,e) Photographs of the device in the initial state (c-DL set on the substrates) (top), the device with the application of the friction force (middle), the device after the removal of the c-DLs. (b,d) Optical microscopy images on the colored parts.

These reference devices were prepared to study the effects of the substrates. A filter paper has suitable roughness to trap the DLs in the device. Therefore, the disruption of DLs induces the outflow of the interior liquid over the substrate.

## Color-changing behavior of PDA and PDA/DL

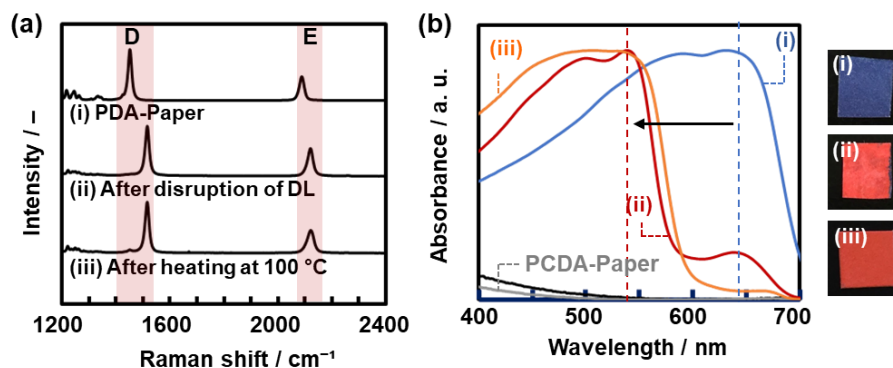


**Fig. S15.** Raman (a) and UV-Vis (b) spectra with the photographs of the PDA-coated paper (i), PDA/DL device after disruption of DL (ii), and PDA with heating at 100 °C (iii).

The color-changing behavior of PDA/DL after disruption of DL was similar to that of PDA with heating. Raman spectra showed the same shift of the peaks corresponding to the ene-yne structure (peaks D and E in Fig. S15a). The red-colored PDA samples showed the similar blue shift of the absorption band in the UV-Vis spectra (Fig. S15b).

## Application of unknown friction force

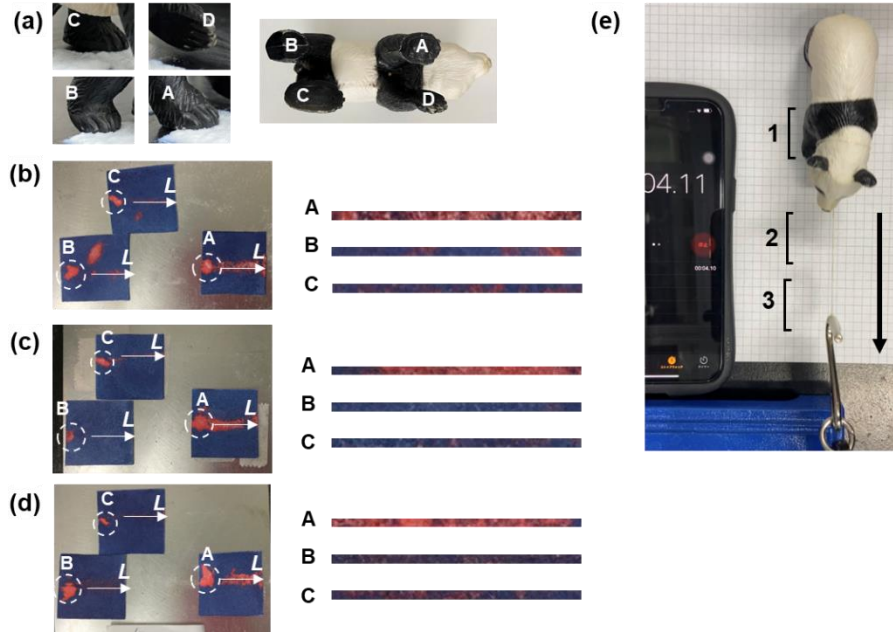


**Fig. S16.** Application of unknown friction force using an ornament of giant panda. (a) Photographs representing the differences in the contact states of four feet. (b–d) Photographs of the devices after the application of friction force in the  $L$ -axis. The experiment was carried out three times to ensure the reproducibility. (e) Setup for measuring the sliding speed of the panda.

**Table S9.** Summary of  $F$  and  $\Delta x$  of PDA/DL under the feet A–C.

|                           | A        | B        | C        | $F_{A-C}$ | $F_s$  |
|---------------------------|----------|----------|----------|-----------|--------|
| (i) $\Delta x / -$        | 0.094179 | 0.022936 | 0.032174 | 0.1730    | N. A.  |
| (ii) $\Delta x / -$       | 0.099534 | 0.007316 | 0.032176 | 0.1610    | N. A.  |
| (iii) $\Delta x / -$      | 0.100638 | 0.02997  | 0.035875 | 0.1931    | N. A.  |
| $\overline{\Delta x} / -$ | 0.098117 | 0.020074 | 0.033408 | 0.1757    | N. A.  |
| S. D. / -                 | 0.002821 | 0.009468 | 0.001744 | 0.0132    | N. A.  |
| Estimated $F / N$         | 0.114159 | 0.022994 | 0.03857  | N. A.     | 0.1687 |

The sliding speed of giant panda was measured in the intervals 1, 2, and 3 as shown in Figure S16a. The average speed in these three intervals was  $6.33 \pm 0.49$ ,  $6.23 \pm 0.32$ , and  $6.12 \pm 0.52$   $\text{cm s}^{-1}$  for the three trials. Therefore, the average speed was estimated to be  $6.2 \pm 0.1$   $\text{cm s}^{-1}$ .



## Application of unknown friction force in calligraphy

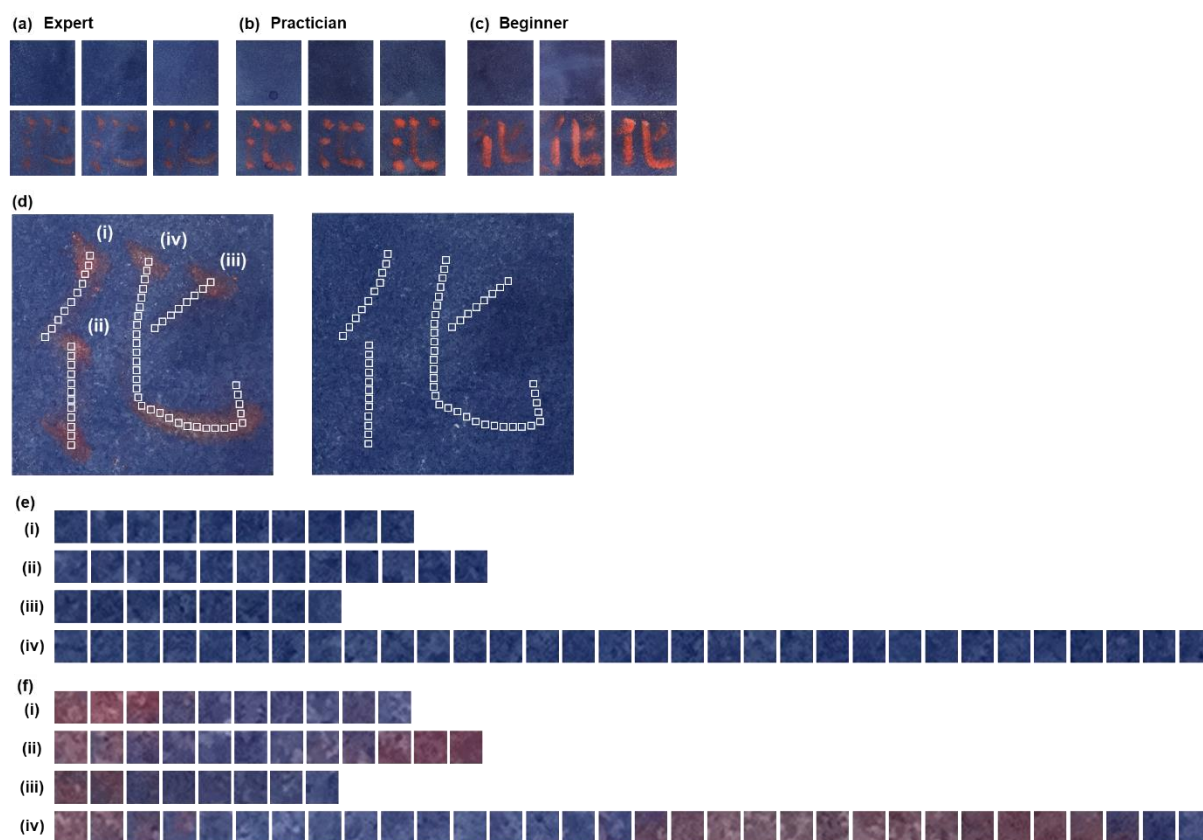


**Fig. S17.** Application of unknown friction force by calligraphy. (a–c) Photographs of the initial state (upper) and color-changed state with the handwriting (lower) by expert (a), practitioner (b), and beginner (c). (d) Segmentalization of the original (right) and color-changed device (left) into 62 domains ( $0.5 \text{ mm} \times 0.5 \text{ mm}$ ) to estimate  $\Delta x$  in the strokes (i)–(iv). (e, f) Photographs of each domain in the initial state (e) and color-changed state with the handwriting in four strokes (i)–(iv) (f).

The  $\Delta x$  values were calculated on each domain using the photographs in Fig. S17e, f.

**Force-distribution mapping using a rigid undeformed pen**

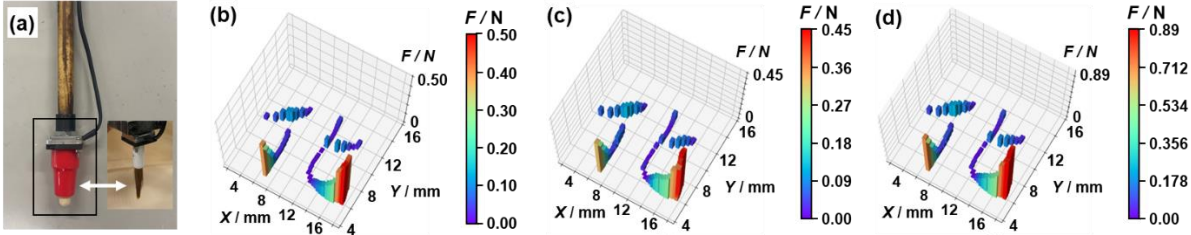


**Fig. S18.** Reference force-distribution mapping using a force sensor for the expert. (a) Experimental setup. (b)  $(F_x^2 + F_y^2)^{0.5}$ . (c)  $F_z$ . (d)  $(F_x^2 + F_y^2 + F_z^2)^{0.5}$ .

The tip of the sensor was exchangeable, as shown in Fig. S18a. The reference sensing experiment was performed using a rigid undeformed pen, whereas the soft brush deformed during writing.